HHS Public Access

Author manuscript

Am J Sports Med. Author manuscript; available in PMC 2022 June 20.

Published in final edited form as:

Am J Sports Med. 2022 June ; 50(7): 1919–1927. doi:10.1177/03635465221090645.

A Novel Model of Hip Femoroacetabular Impingement in Immature Rabbits Reproduces the Distinctive Head-Neck Cam Deformity

Tomoyuki Kamenaga, MD, PhD[*],

Masahiko Haneda, MD, PhD[†],

Robert H. Brophy, MD[*],

Regis J. O'Keefe, MD, PhD[*],

John C. Clohisy, MD[*],

Cecilia Pascual-Garrido, MD, PhD[*,‡]

[*]Washington University School of Medicine, St Louis, Missouri, USA.

[†]Hyogo Rehabilitation Center, Kobe, Japan.

Abstract

Background: Femoroacetabular impingement (FAI) is a leading cause of hip pain in young adults and often leads to degenerative osteoarthritis (OA). A small animal model of hip deformities is crucial for unraveling the pathophysiology of hip OA secondary to FAI.

Purposes: To (1) characterize a new minimally invasive surgical technique to create a proximal femoral head-neck deformity in a skeletally immature rabbit model and (2) document the effect of an injury to the medial proximal femoral epiphysis on head-neck morphology at 28 days after the injury.

Study Design: Controlled laboratory study.

Methods: Six-week-old New Zealand White rabbits (n = 10) were subjected to right hip surgery, with the left hip used as a control. An epiphyseal injury in the medial femoral head was created using a 1.6-mm drill. Hips were harvested bilaterally at 28 days after surgery. Alpha and epiphyseal shaft angles were measured on radiographs. Alpha angles at the 1- and 3-o'clock positions were measured on the oblique axial plane of micro–computed tomography images. Bone

[‡]Address correspondence to Cecilia Pascual-Garrido, MD, PhD, Washington University School of Medicine, 660 South Euclid Avenue, MSC 8233-0004-5505, St Louis, MO 63110, USA (cpascualgarrido@wustl.edu).

Investigation performed at Washington University School of Medicine, St Louis, Missouri, USA

One or more of the authors has declared the following potential conflict of interest or source of funding: This study was supported in part by a National Institutes of Health K08 Clinical Investigator Award (1K08AR077740-01) and an Orthopaedic Research and Education Foundation Mentored Clinician-Scientist Grant. The Curing Hip Disease Fund and the Jackie and Randy Baker Research Fellowship provided partial support for the research personnel. R.H.B. has received consulting fees from Sanofi, support for education from Elite Orthopaedics and Arthrex, and speaking fees from Arthrex. J.C.C. has received research support from Zimmer Biomet; consulting fees from MicroPort Orthopedics, Smith & Nephew, and Zimmer Biomet; royalties from Wolters Kluwer Health and Zimmer Biomet; and speaking fees from Synthes. C.P.-G. has received grants from Sanofi and Zimmer Biomet, support for education from Elite Orthopaedics, and hospitality payments from Zimmer Biomet and Stryker. AOSSM checks author disclosures against the Open Payments Database (OPD). AOSSM has not conducted an independent investigation on the OPD and disclaims any liability or responsibility relating thereto.

bar formation secondary to growth plate injuries was confirmed using alcian blue hematoxylin staining.

Results: All hips in the study group showed a varus-type head-neck deformity, with lower epiphyseal shaft angles on anteroposterior radiographs versus those in the control group (133° ± 8° vs 142° ± 5°, respectively; $P = .022$) and higher epiphyseal shaft angles on lateral radiographs (27° ± 12° vs 10° ± 7°, respectively; $P < .001$). The mean alpha angles in the study group were higher at both the 1- (103° ± 14° vs 46° ± 7°, respectively; $P < .002$) and 3-o'clock (99° ± 18° vs 35° ± 11°, respectively; $P < .002$) positions than those in the control group. Alcian blue hematoxylin staining of all hips in the study group indicated that the injured physis developed a bony bar, leading to growth plate arrest on the medial femoral head.

Conclusion: The proposed model led to growth arrest at the proximal femoral physis, resulting in a femoral head-neck deformity similar to human FAI.

Clinical Relevance: Our novel small animal model of a femoral head-neck deformity is a potential platform for research into the basic mechanisms of FAI disease progression and the development of disease-modifying therapies.

Keywords

femoroacetabular impingement; animal model; immature rabbit; head-neck deformity

Femoroacetabular impingement (FAI) has been established as an important cause of hip osteoarthritis (OA).[7] Today, FAI is recognized as a leading cause of hip pain in younger adults as well as degenerative arthritis in the hip.[4] The estimated prevalence of FAI has varied between 10% and 25% in the population.[13] Detailed characterizations of abnormal bone morphology, intra-articular disease, and clinical risks for the disease progression of FAI have been extensively reported.[14,16,18,20,33] Recent molecular analyses identified an inflammatory cascade in FAI using cartilage samples from the impingement zone of the hip in patients undergoing surgical treatment for symptomatic FAI, suggesting that the impingement area is metabolically active and a potential structural precursor to hip OA.[8,9] However, the basic biological mechanisms of disease in FAI remain unknown.

Animal models can serve as platforms to study the mechanism of disease and the efficacy of potential treatment options. To date, there have been limited animal models of hip OA secondary to FAI. Recently, an article published by Killian et al[15] reported on a murine model of hip instability. Up to now, there has been only 1 reported large animal model of experimentally induced hip FAI in sheep[28,34] in which a deformity was created via intertrochanteric varus osteotomy. Large animal models are attractive, but they are expensive and not as widely available as small animal models. Human patterns of proximal femoral deformities have been reported,[29] showing that the resulting head deformity depends specifically on the location of the femoral head epiphyseal injury. Asymmetric epiphyseal closure due to unequal loading during intense physical activity has been shown to result in angular deformities of the femoral head-neck junction in adolescent athletes.[1,5] Additionally, a previous article regarding epiphysiodesis of the femoral head growth plate reported that partial medial epiphysiodesis results in medial physis growth arrest but allows normal lateral growth of the longitudinal growth plate, eventually tilting the femoral head to

varus.[29] Therefore, one plausible approach to creating a head-neck deformity similar to that observed in cam-type FAI is to intentionally create an injury to the medial third of the proximal femoral epiphysis of an immature hip. One of the indicators used in evaluating deformities at the femoral head-neck junction is the alpha angle: an alpha angle of >55° is considered indicative of cam-type FAI.[11,19] Another indicator is the Southwick angle,[31] which is clinically used for the assessment of a slipped capital femoral epiphysis. This angle can be used to evaluate the tilt of the femoral head relative to the femoral shaft.[21,25] Recent 3-dimensional imaging studies have measured the alpha angle in the oblique axial plane using a clockface system to identify morphological abnormalities of the femoral neck and acetabulum on computed tomography (CT) or magnetic resonance imaging scans of the proximal femur.[22,23] A cam-type deformity is most noticeable at the 1- to 3-o'clock positions corresponding to the anterosuperior region of the femoral head-neck junction.[22,23] Thus, the oblique axial view using a clockface produces useful morphological information beyond that offered by radiography.

The purposes of the current study were to (1) characterize a new minimally invasive surgical technique to create a proximal femoral head-neck deformity in a skeletally immature rabbit model and (2) document the effect of an injury to the medial proximal femoral epiphysis on head-neck morphology in the oblique axial plane of CT images at 28 days after the injury. We hypothesized that an intentional injury to the proximal femoral physis of immature hips would result in a bone bridge or asymmetric growth arrest and a secondary cam-type deformity at the femoral head-neck junction.

METHODS

Animal Model

We used 6-week-old immature New Zealand White rabbits. A total of 10 rabbits were used and subjected to right hip surgery. The contralateral left hip was used as a control (nonsurgical). Baseline radiography was performed before surgery, and postoperative radiography was conducted at 28 days in euthanized rabbits. This study received approval from the hospital and university Institutional Animal Care and Use Committee (#20190071). The study design is summarized in Figure 1.

Surgical Procedure

The 6-week-old immature New Zealand White rabbits were anesthetized via an intramuscular injection of ketamine (35 mg/kg) and xylazine (5 mg/kg), followed by isoflurane inhalation (3%–5% isoflurane; 2–3 minutes for induction and then maintained at 1.5%–3% via a nose cone). The following analgesics were given at induction: 0.05 mg/kg of buprenorphine subcutaneously and 0.3 mg/kg of meloxicam subcutaneously. Anesthesia was administered under veterinary supervision by an anesthetic technician. After the induction of general anesthesia, anteroposterior (AP) pelvis and frog lateral radiographs were taken with rabbits on the operating table in the supine position immediately before surgery.

The site of surgery was shaved, prepared, and draped in a standard sterile fashion, ensuring that the proximal thigh was exposed in the field. A 4-cm straight incision was made on the

lateral aspect of the right hip joint and carried through the subcutaneous tissue. The lateral fascia was cut, and the tensor fasciae latae muscle and gluteus muscle were retracted. The hip capsule was identified, and T-shaped capsulotomy was performed. After capsulotomy was performed, hip traction was applied by pulling the lower extremity to distract the joint, allowing full exposure of the femoral head (Figure 2A). After the femoral epiphysis was identified, the femoral head was measured using a ruler, and the medial third of the epiphysis was marked using a marking pen. A 3 × 2 × 6–mm defect in the epiphysis was created via drilling using a 1.6-mm drill bit (Figure 2B). To attain the proper depth, we attached a stopper at 6 mm from the tip of the drill. The intraoperative location of the epiphyseal injury was successfully identified by measuring the size of the femoral head from medial to lateral and then finding the medial third. To achieve an appropriate drill direction, we held the rotary tool at a proper angle of 30° with respect to the femoral diaphysis. After the hip joint was irrigated profusely, the capsule, fasciae, and skin were closed using sutures in separate layers. To confirm that there was no postoperative residual instability, we conducted a manual test, taking the hip through extreme ranges of motion and performing distraction of the hip joint. The injury model is shown in Figure 3.

After the procedure, the animals underwent AP pelvis radiography to confirm the presence of a bony defect at the injury site. Animals were then allowed to bear weight as tolerated. The protocol (with modification) is based on the femoral head osteonecrosis model reported by Tudisco et al.[32] The contralateral left hip did not undergo any intervention and served as a control. At 28 days after surgery, the animals were euthanized, and both hips underwent radiography and were harvested.

Radiographic Assessment of Head-Neck Deformity

Radiographically, the Southwick and alpha angles were used to assess the head-neck deformity. The Southwick angle is used to measure the epiphyseal shaft angle and was assessed on both AP pelvis and frog lateral radiographs as previously described (preoperatively and 28 days after surgery)[21,31] (Figure 4). To assess the varus tilt of the injured femoral head, we calculated the difference in the epiphyseal shaft angle in the AP pelvis view between the control and study hips (“value in control hip” minus “value in study hip”),[21] and considered a positive value to indicate varus tilt of the femoral head. The alpha angle was also measured, as described by Nötzli et al,[19] on AP pelvis and frog lateral radiographs.

Micro-CT

All hips (n = 20) were scanned using a vivaCT 40 micro-CT scanner (70 kVp, 114 μA, 100-millisecond integration time, 30-μm resolution; Scanco Medical) for analysis of the deformity of the femoral head and the bony structure, including the epiphyseal line or physis. The deformity of the femoral head was assessed by measuring the alpha angle according to previous reports.[3,23] Multiplanar reformation (MPR) was carried out to generate oblique axial and oblique sagittal plane images, parallel and perpendicular to the long axis of the femoral neck, respectively. Radial MPR images were constructed with the axis of rotation as the center of the femoral neck while cross-referencing to the oblique sagittal plane, showing the femoral neck in the short axis. The most superior point of the

femoral head-neck junction was defined as 12 o'clock using clockface nomenclature (Figure 5A). Acquired MPR images were analyzed using ImageJ software (National Institutes of Health), and the alpha angles were measured in the oblique axial plane at the 1- (Figure 5B) and 3-o'clock positions (Figure 5C), representing the anterolateral and direct anterior positions, respectively.

Histology

Both hips were fixed in 10% neutral buffered formalin for 24 to 48 hours, dehydrated, embedded in paraffin wax, and sectioned (5 μm). Deparaffinized coronal sections of the femoral head were stained with alcian blue hematoxylin and orange G/eosin counterstaining,[26] which stains cartilage tissue blue, bone tissue bright orange, fibrous tissue pink, and hematopoietic/marrow tissue dark purple, to analyze histological features of the femoral epiphysis and bone bridge formation.

Statistical Analysis

High intraobserver and interobserver reliability of the epiphyseal shaft angle on radiographic analysis of the slipped capital femoral epiphysis in humans have previously been reported.[10] Additionally, we calculated intraclass and interclass correlation coefficients, finding good reliability between readers. All measurements were performed twice by one examiner and once by another examiner. All values are presented as mean ± standard deviation. Data analysis was conducted using JMP 14 (SAS Institute). The Wilcoxon signed rank test was used to compare quantitative variables between the study and control groups. $P < .05$ indicated statistically significant differences. An a priori power calculation for the Wilcoxon signed rank test with paired samples was performed using G*Power 3.[6] To detect an effect size of 1.0 with a 2-tailed alpha level of .05 and beta of 0.2, the estimated sample size was 10 rabbits (20 hips).

RESULTS

Representative micro-CT and histological images of the femoral head are shown in Figure 6. At 28 days after the injury, medial epiphyseal closure with an anteromedial femoral head prominence in the study group was observed in all rabbits (10/10; 100%) (Figure 6, A and B), whereas the femoral heads of all rabbits in the control group showed an intact epiphyseal line without a secondary femoral head deformity (Figure 6, C and D). On histological examination using alcian blue hematoxylin staining, the physeal injury was apparent with the epiphyseal bone extending through the physeal line and into the metaphyseal bone in all hips of the study group. Injured physes had a dense bony bar at the injury site and resulted in growth plate disruption with closure of the epiphyseal line on the medial aspect of the femoral head (Figure 6, E and F). In contrast, there was no evidence of physeal arrest, and intact continuous physeal cartilage was observed in all specimens of the control group (Figure 6, G and H).

Radiographic Assessment of Head-Neck Deformity

Radiographic results are summarized in Table 1. Radiographs taken at 28 days after the injury demonstrated that hips in the study group (right hips) had a varus tilt and an

anteromedial prominence of the femoral head. The study group, compared with the control group, showed a varus tilt of the femoral head with a lower epiphyseal shaft angle on the AP radiographic view (difference, 9.3° ± 4.9° [range, 3.4° -15.8°]; $P = .022$) and confirmed asphericity of the femoral head with a higher alpha angle ($P < .001$) (Figure 7A). Additionally, an anterior protrusion of the femoral head with a higher epiphyseal shaft angle was evident on the lateral radiographic view ($P < .001$) (Figure 7B).

Assessment of Head-Neck Deformity Using Micro-CT

Using Micro-CT, we confirmed a cam-type deformity in the injured femoral head (study group), with higher alpha angles than those in control hips in the oblique axial plane at the 1-and 3-o'clock positions ($P = .002$) (Table 2). On representative 3-dimensional micro-CT images, we confirmed that the injured femoral head resulted in a varus tilt of the femoral head with an aspherical anteromedial and anterolateral surface (Figure 7C).

DISCUSSION

Hip FAI continues to have a major role in the development of hip OA.[24] Since the FAI concept was refined by Ganz and colleagues,[7] tremendous advances in the characterization of abnormal bone morphology, intra-articular disease, and clinical risks for disease progression have been reported.[14,16,18,20,33] In addition to the discovery of human pathological pathways of hip OA, developing a small animal model of hip deformities is crucial for unraveling the complex pathophysiology of hip OA and testing the efficacy of potential therapeutic interventions.

Our proposed novel animal model achieved a bony bridge and/or growth arrest at the proximal femoral physis and led to a head-neck deformity at the anteromedial aspect of the femoral head and a secondary deformity at the anterosuperior aspect of the femoral head, similar to that observed in human hip FAI. To our knowledge, the only animal model of hip FAI that has been reported is in large mature sheep by performing extra-articular varus closing wedge hip osteotomy.[28] Our proposed model differs from this previously described animal model. First, our model utilizes an immature skeleton and directly injures the open physis, resulting in a bone bridge. We believe that this better re-creates the physiopathology of a hip cam FAI deformity. Previously, it has been shown that a head-neck deformity with cam FAI morphology develops during the growth period in adolescent athletes,[1,27] secondary to asymmetric closure of the capital femoral epiphysis because of unequal loading during intense physical activity.[5] Moreover, a young in vitro porcine animal model has been used to investigate the effect of cyclic loading on the immature femoral head.[12] The authors confirmed that chronic vertical loading on the young porcine proximal femur results in microscopic injuries to the physeal plate.[12] Interestingly, their histological findings were similar to ours, with a physeal injury running perpendicular to the physeal line. Furthermore, our model utilizes a small animal, which is advantageous because it is a widely used breed, has a short life cycle, and is economical compared with the expenses associated with large animals.[17]

The bone deformity was confirmed radiographically and on micro-CT images. Varus tilt of the femoral head and asphericity at the anterosuperior aspect of the femoral head-neck area

developed, and they were similar to those observed in cam FAI morphology. Although we have not yet confirmed that this induced head-neck deformity will result in a macroscopic damage pattern similar to that observed in hip FAI, we believe that with an additional longer follow-up, we would observe a typical pattern of intra-articular lesions.[20] In a previous study, experimentally induced cam impingement in sheep[34] via intertrochanteric varus osteotomy resulted in a cam-type deformity of the femoral head. The authors showed that contrary to in humans, impingement occurred at the posterosuperior aspect of the acetabulum. The difference in location is explained by the upright walking pattern in humans as opposed to the quadrupedal motion pattern in sheep.[34] We believe that in a rabbit model, induced FAI impingement will result in a similar pattern of intra-articular disease as observed in sheep. A future long-term follow-up is needed to confirm the intra-articular pattern of disease.

Our animal model had a number of limitations. First, the animals were euthanized at 28 days; thus, we could not assess for intra-articular lesions and the progression to OA that may occur with time. However, our aim, in this first phase of the experiment, was to characterize the head-neck deformity resulting from a physeal injury. In the near future, we will proceed with a longer follow-up analysis to assess the progression of intra-articular disease. We expect that as the rabbits continue to grow, the deformity will progress in severity, and secondary intra-articular damage with a progression to OA will be evident. Second, our report was based on an observational approach only. We did not provide information about joint mechanics or contact stress magnitudes that could confirm that this deformity impinges on the acetabulum. In the future, when the animals are kept longer, we will be able to predict the zone of conflict between the abnormal head-neck junction and acetabulum using a simulated computer-based range of motion. Third, the injury model involved opening the capsule and creating an intra-articular injury. This model may produce a direct inflammatory or humoral factor response that may arise from the synovium after intra-articular penetration. We acknowledge that this acute inflammation due to surgical invasion may not mimic human FAI. However, we believe that this acute inflammation should significantly calm down at 2 weeks after the procedure. A previous article on an experimentally induced OA animal model reported that initial inflammation due to surgical damage went down by 2 weeks after surgery.[30] Additionally, there have been multiple previously accepted models of OA that involved intra-articular approaches.[2,30]

This study presents a novel rabbit model of hip FAI. The proposed model led to growth arrest at the proximal femoral physis, resulting in a femoral head-neck deformity similar to human FAI. Further studies will be needed to confirm if this model could be a potential platform for further research into hip FAI disease progression and testing the efficacy of therapeutic interventions.

ACKNOWLEDGMENT

The authors thank May Wu, Crystal Idleburg, and Samantha Coleman for their technical assistance as well as Chadi Nahal, Gail E. Pashos, Sean M. Akers, Caroline Drain, and Karla J. Crook for their assistance.

REFERENCES

1. Agricola R, Heijboer MP, Ginai AZ, et al. A cam deformity is gradually acquired during skeletal maturation in adolescent and young male soccer players: a prospective study with minimum 2-year follow-up. Am J Sports Med. 2014;42(4):798–806. [PubMed: 24585362]
2. Bansal S, Miller LM, Patel JM, et al. Transection of the medial meniscus anterior horn results in cartilage degeneration and meniscus remodeling in a large animal model. J Orthop Res. 2020;38(12): 2696–2708. [PubMed: 32285971]
3. Beaule PE, Speirs AD, Anwander H, et al. Surgical correction of cam deformity in association with femoroacetabular impingement and its impact on the degenerative process within the hip joint. J Bone Joint Surg Am. 2017;99(16):1373–1381. [PubMed: 28816897]
4. Beck M, Kalhor M, Leunig M, Ganz R. Hip morphology influences the pattern of damage to the acetabular cartilage: femoroacetabular impingement as a cause of early osteoarthritis of the hip. J Bone Joint Surg Br. 2005;87(7):1012–1018. [PubMed: 15972923]
5. Cho YJ, Jung GY, Kim EJ, Chun YS, Rhyu KH. Asymmetric epiphyseal closure of the femoral head as a potential cause of the primary cam lesion: a case report. Skeletal Radiol. 2016;45(9):1299–1302. [PubMed: 27255537]
6. Faul F, Erdfelder E, Buchner A, Lang AG. Statistical power analyses using G*Power 3.1: tests for correlation and regression analyses. Behav Res Methods. 2009;41(4):1149–1160. [PubMed: 19897823]
7. Ganz R, Parvizi J, Beck M, et al. Femoroacetabular impingement: a cause for osteoarthritis of the hip. Clin Orthop Relat Res. 2003;417:112–120.
8. Haneda M, Rai MF, O'Keefe RJ, et al. Inflammatory response of articular cartilage to femoroacetabular impingement in the hip. Am J Sports Med. 2020;48(7):1647–1656. [PubMed: 32383968]
9. Hashimoto S, Rai MF, Gill CS, et al. Molecular characterization of articular cartilage from young adults with femoroacetabular impingement. J Bone Joint Surg Am. 2013;95(16):1457–1464. [PubMed: 23965695]
10. Herngren B, Lindell M, Hägglund G. Good inter- and intraobserver reliability for assessment of the slip angle in 77 hip radiographs of children with a slipped capital femoral epiphysis. Acta Orthop. 2018;89(2):217–221. [PubMed: 29212388]
11. Johnston TL, Schenker ML, Briggs KK, Philippon MJ. Relationship between offset angle alpha and hip chondral injury in femoroacetabular impingement. Arthroscopy. 2008;24(6):669–675. [PubMed: 18514110]
12. Jónasson PS, Ekström L, Hansson HA, et al. Cyclical loading causes injury in and around the porcine proximal femoral physeal plate: proposed cause of the development of cam deformity in young athletes. J Exp Orthop. 2015;2(1):6. [PubMed: 26914874]
13. Jung KA, Restrepo C, Hellman M, et al. The prevalence of cam-type femoroacetabular deformity in asymptomatic adults. J Bone Joint Surg Br. 2011;93(10):1303–1307. [PubMed: 21969426]
14. Kemp J, Grimaldi A, Heerey J, et al. Current trends in sport and exercise hip conditions: intra-articular and extra-articular hip pain, with detailed focus on femoroacetabular impingement (FAI) syndrome. Best Pract Res Clin Rheumatol. 2019;33(1):66–87. [PubMed: 31431276]
15. Killian ML, Locke RC, James MG, et al. Novel model for the induction of postnatal murine hip deformity. J Orthop Res. 2019;37(1):151–160. [PubMed: 30259572]
16. Louer CR, Pashos G, Clohisy JC, Nepple JJ. A prospective analysis of the contralateral hip among patients with femoroacetabular impingement: what are the risk factors for disease progression? Am J Sports Med. 2018;46(10):2486–2491. [PubMed: 30015502]
17. Mapara M, Thomas BS, Bhat KM. Rabbit as an animal model for experimental research. Dent Res J (Isfahan). 2012;9(1):111–118. [PubMed: 22363373]
18. Morris WZ, Li RT, Liu RW, Salata MJ, Voos JE. Origin of cam morphology in femoroacetabular impingement. Am J Sports Med. 2018;46(2):478–486. [PubMed: 28334547]
19. Nö tzli HP, Wyss TF, Stoecklin CH, et al. The contour of the femoral head-neck junction as a predictor for the risk of anterior impingement. J Bone Joint Surg Br. 2002;84(4):556–560. [PubMed: 12043778]

20. Pascual-Garrido C, Li DJ, Grammatopoulos G, et al. The pattern of acetabular cartilage wear is hip morphology-dependent and patient demographic-dependent. Clin Orthop Relat Res. 2019;477(5):1021–1033. [PubMed: 30998630]
21. Peck DM, Voss LM, Voss TT. Slipped capital femoral epiphysis: diagnosis and management. Am Fam Physician. 2017;95(12):779–784. [PubMed: 28671425]
22. Pfirrmann CW, Mengiardi B, Dora C, et al. Cam and pincer femoroacetabular impingement: characteristic MR arthrographic findings in 50 patients. Radiology. 2006;240(3):778–785. [PubMed: 16857978]
23. Rakhra KS, Sheikh AM, Allen D, Beaule PE. Comparison of MRI alpha angle measurement planes in femoroacetabular impingement. Clin Orthop Relat Res. 2009;467(3):660–665. [PubMed: 19037709]
24. Sankar WN, Nevitt M, Parvizi J, et al. Femoroacetabular impingement: defining the condition and its role in the pathophysiology of osteoarthritis. J Am Acad Orthop Surg. 2013;21(suppl 1):S7–S15. [PubMed: 23818194]
25. Santili C, de Assis MC, Kusabara FI, et al. Southwick's head-shaft angles: normal standards and abnormal values observed in obesity and in patients with epiphysiolysis. J Pediatr Orthop B. 2004;13(4): 244–247. [PubMed: 15199279]
26. Sayers DC, Volpin G, Bentley G. The demonstration of bone and cartilage remodelling using alcian blue and hematoxylin. Stain Technol. 1988;63(1):59–63. [PubMed: 2451328]
27. Siebenrock KA, Ferner F, Noble PC, et al. The cam-type deformity of the proximal femur arises in childhood in response to vigorous sporting activity. Clin Orthop Relat Res. 2011;469(11):3229–3240. [PubMed: 21761254]
28. Siebenrock KA, Fiechter R, Tannast M, Mamisch TC, von Rechenberg B. Experimentally induced cam impingement in the sheep hip. J Orthop Res. 2013;31(4):580–587. [PubMed: 23447499]
29. Siffert RS. Patterns of deformity of the developing hip. Clin Orthop Relat Res. 1981;160:14–29.
30. Sophocleous A, Huesa C. Osteoarthritis mouse model of destabilization of the medial meniscus. Methods Mol Biol. 2019;1914:281–293. [PubMed: 30729471]
31. Southwick WO. Osteotomy through the lesser trochanter for slipped capital femoral epiphysis. J Bone Joint Surg Am. 1967;49(5):807–835. [PubMed: 6029256]
32. Tudisco C, Botti F, Bisicchia S, Ippolito E. Ischemic necrosis of the femoral head: an experimental rabbit model. J Orthop Res. 2015;33(4):535–541. [PubMed: 25411023]
33. Yao JJ, Cook SB, Gee AO, Kweon CY, Hagen MS. What is the survivorship after hip arthroscopy for femoroacetabular impingement? A large-database study. Clin Orthop Relat Res. 2020;478(10):2266–2273. [PubMed: 32604156]
34. Zurmuhle CA, Schmaranzer F, Nuss K, et al. Proof of concept: hip joint damage occurs at the zone of femoroacetabular impingement (FAI) in an experimental FAI sheep model. Osteoarthritis Cartilage. 2019;27(7):1075–1083. [PubMed: 30991104]

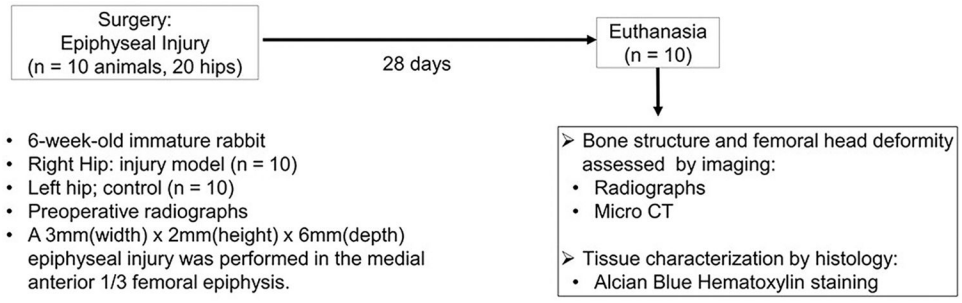

Figure 1.
Study design. CT, computed tomography.

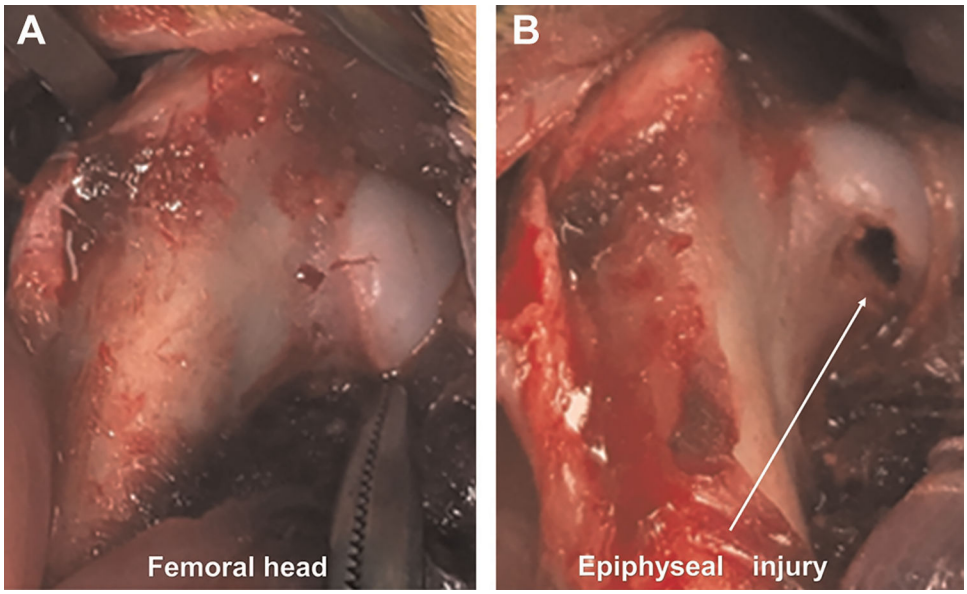

Figure 2.
Surgical steps for a femoral epiphyseal injury in an immature rabbit. (A) The femoral epiphysis is identified after T-shaped capsulotomy. (B) An epiphyseal injury is created using a 1.6-mm drill bit.

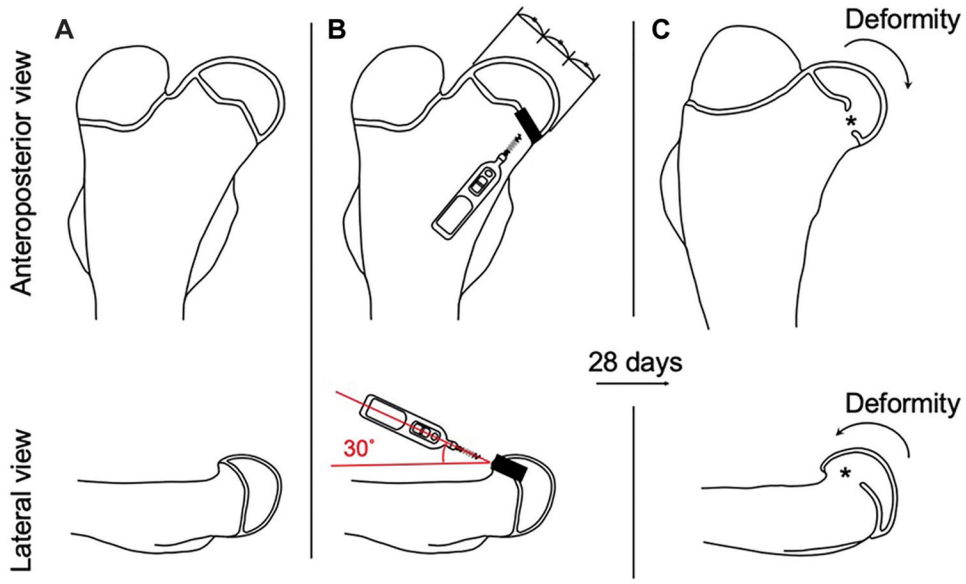

Figure 3.

Injury model. (A) The right hip before an epiphyseal injury. (B) An epiphyseal injury is created using a 1.6-mm drill bit through the anteromedial aspect of the medial third of the femoral head at an angle of 30° with respect to the femoral diaphysis. (C) Damage to the femoral epiphysis results in a deformity of the femoral head at 28 days after surgery.

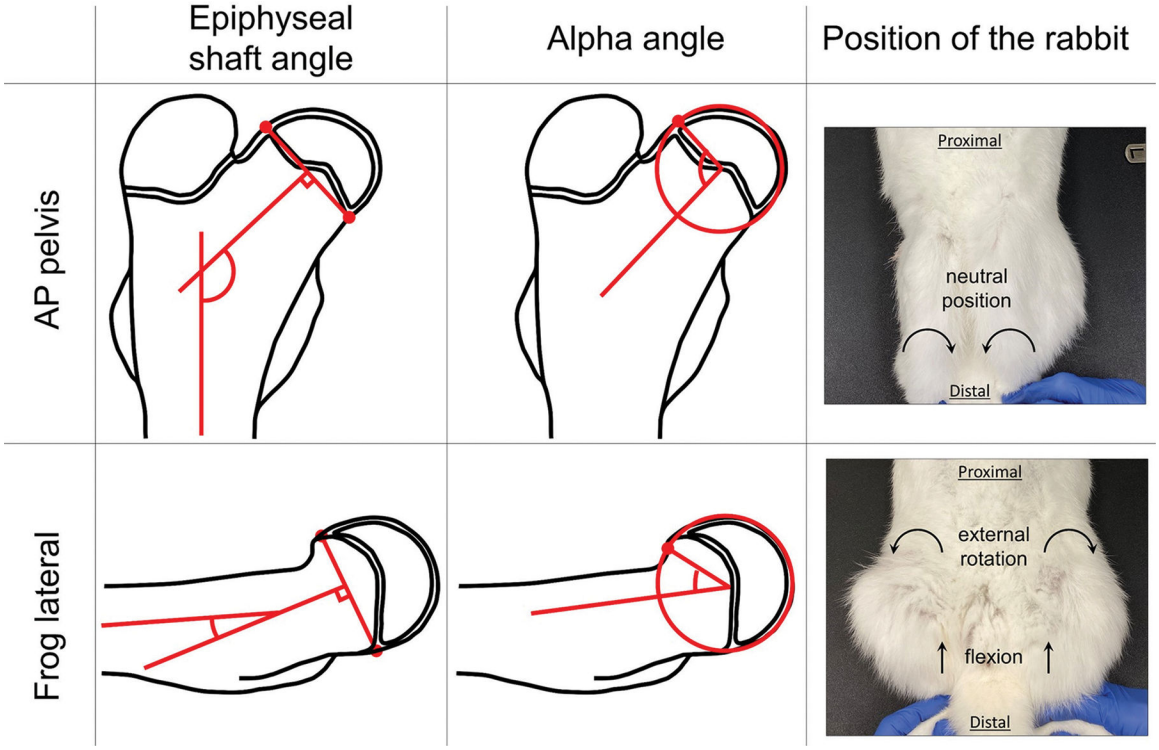

Figure 4.
Methodology used to measure the Southwick and alpha angles on anteroposterior (AP) pelvis and frog lateral radiographs. The position of the rabbit when the radiographs were taken is shown on the right.

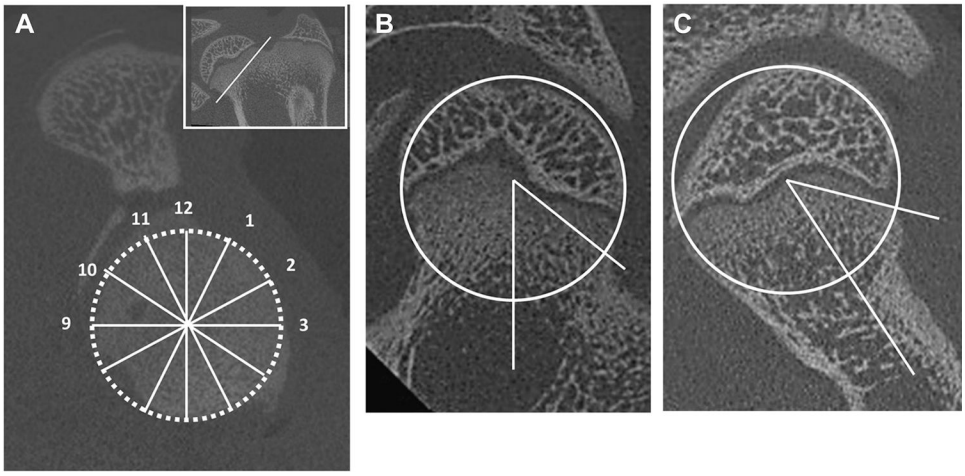

Figure 5.

Measurement of the alpha angle. (A) Multiplanar reformation was used to generate oblique axial plane images with a cross-reference to the oblique sagittal plane, showing the femoral neck in the short axis. The most superior point of the femoral head-neck junction was defined as 12 o'clock using clockface nomenclature. The alpha angle was measured between the femoral neck shaft axis and a line drawn from the femoral head center to the point where the head extended beyond the margin of the best-fit circle at the (B) 1- and (C) 3-o'clock positions.

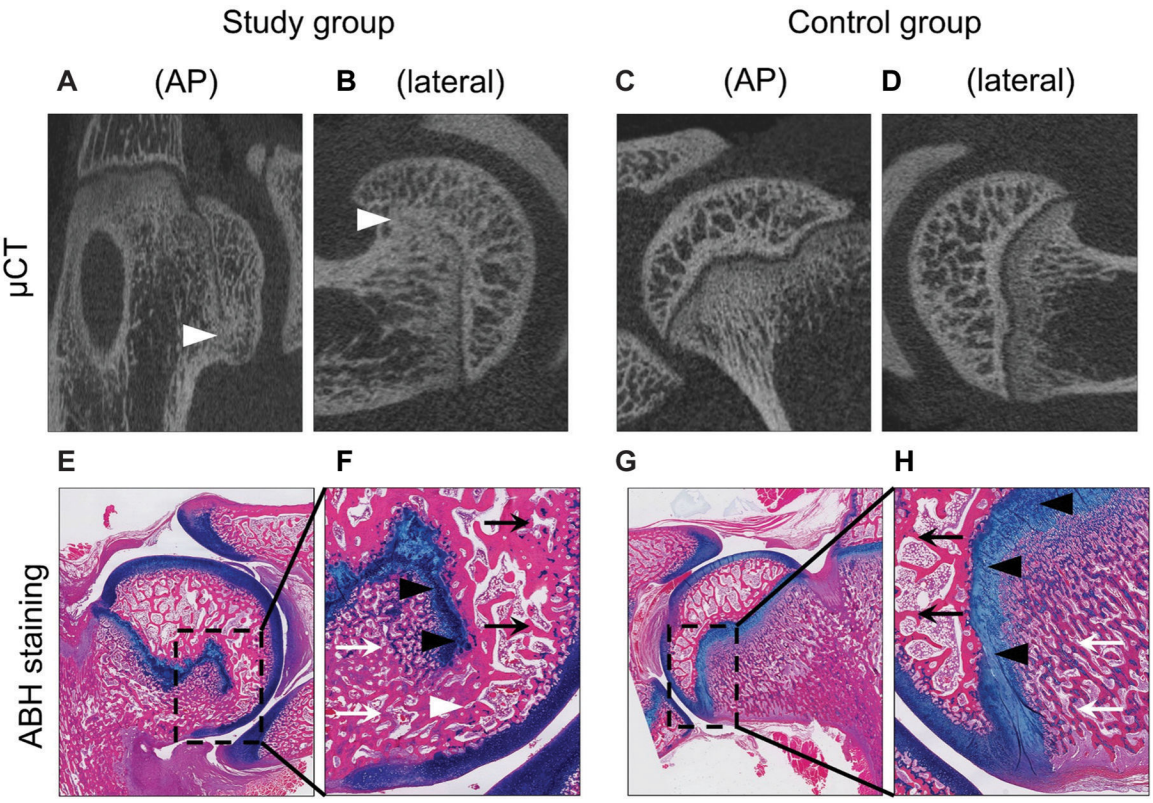

Figure 6.
(A-D) Micro–computed tomography (μ-CT) images and (E-H) alcian blue hematoxylin (ABH) staining of the femoral head in the (A, B, E, F) study group and (C, D, G, H) control group. A bone bridge (white arrowhead) extending from the epiphyseal bone (black arrow) through the physeal line (black arrowhead) and into the metaphyseal bone (white arrow) is seen. AP, anteroposterior.

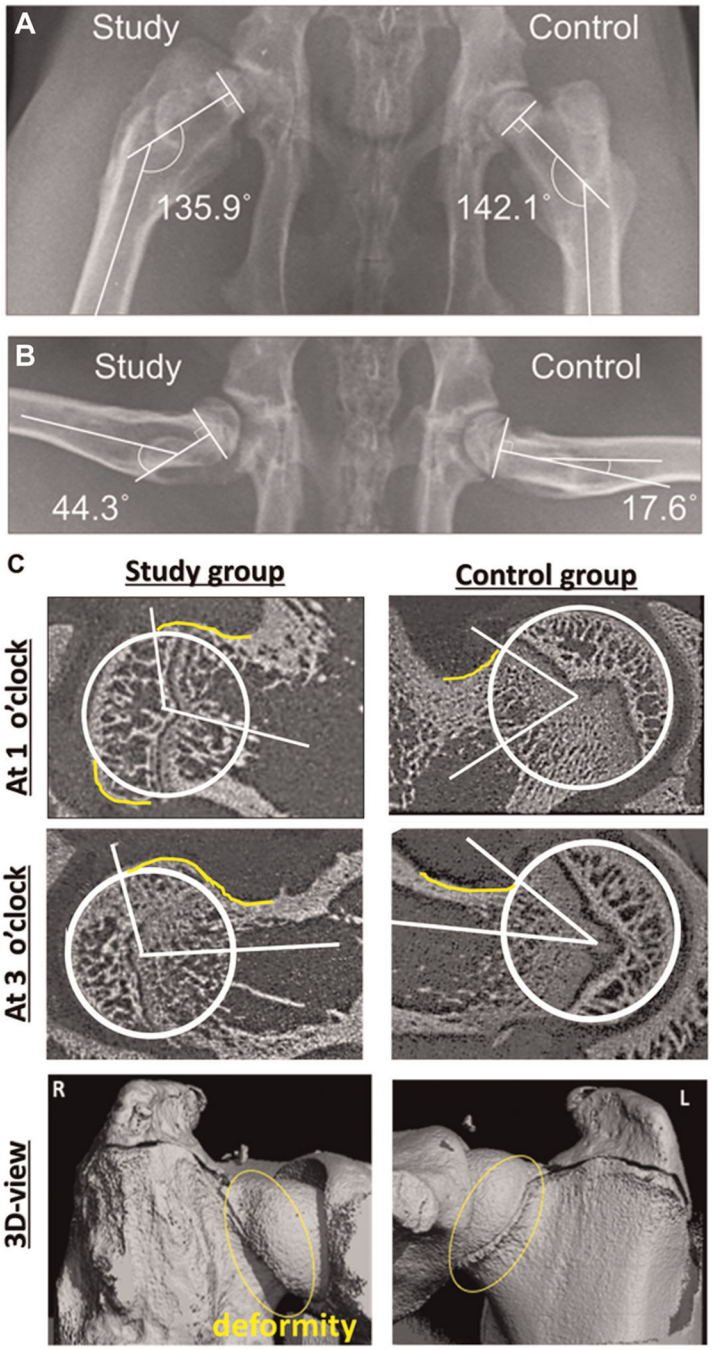

Figure 7.

A head-neck deformity on (A) anteroposterior pelvis and (B) frog lateral radiographs with the epiphyseal shaft angle. (C) A 3-dimensional reconstruction section on micro–computed tomography images showing the 1- and 3-o'clock positions of the femoral head-neck junction.

TABLE 1

Radiographic Findings of Hip Deformities[a]

	Control Group (n = 10)	Study Group (n = 10)	*P* Value	Intraclass Correlation Coefficient	Interclass Correlation Coefficient
Southwick angle, deg					
AP	142.0 ± 4.7	132.7 ± 8.3	.022	0.83	0.84
Lateral	9.6 ± 6.6	26.9 ± 12.2	<.001	0.88	0.90
Alpha angle, deg					
AP	57.6 ± 8.1	110.4 ± 14.1	<.001	0.85	0.82
Lateral	37.1 ± 6.4	101.4 ± 24.7	<.001	0.95	0.96

[a]Data are reported as mean ± SD. AP, anteroposterior.

TABLE 2

Alpha Angles on Micro–Computed Tomography Images[a]

	Control Group (n = 10)	Study Group (n = 10)	*P* Value	Intraclass Correlation Coefficient	Interclass Correlation Coefficient
Alpha angle at 1 o'clock, deg	45.6 ± 7.3	102.8 ± 13.7	.002	0.82	0.86
Alpha angle at 3 o'clock, deg	35.4 ± 10.6	98.6 ± 17.7	.002	0.85	0.84

[a]Data are reported as mean ± SD.